

Refractive index and hygroscopic stability of $\text{Al}_x\text{Ga}_{1-x}\text{As}$ native oxides

D. C. Hall,^{a)} H. Wu, L. Kou, Y. Luo, and R. J. Epstein

Department of Electrical Engineering, University of Notre Dame, Notre Dame, Indiana 46556

O. Blum and H. Hou

Sandia National Laboratory, Albuquerque, New Mexico 87185

(Received 17 May 1999; accepted for publication 25 June 1999)

We present prism coupling measurements on $\text{Al}_x\text{Ga}_{1-x}\text{As}$ native oxides showing the dependence of refractive index on composition ($0.3 \leq x \leq 0.97$), oxidation temperature ($400 \leq T \leq 500$), and carrier gas purity. Index values range from $n = 1.490$ ($x = 0.9$, 400°C) to 1.707 ($x = 0.3$, 500°C). The oxides are shown to adsorb moisture, increasing their index by up to 0.10 (7%). Native oxides of $\text{Al}_x\text{Ga}_{1-x}\text{As}$ ($x \leq 0.5$) have index values up to 0.27 higher and are less hygroscopic when prepared with a small amount of O_2 in the $\text{N}_2 + \text{H}_2\text{O}$ process gas. The higher index values are attributed to a transition from a hydroxide to a denser $(\text{Al}_x\text{Ga}_{1-x})_2\text{O}_3$ oxide phase. © 1999 American Institute of Physics. [S0003-6951(99)00434-9]

Numerous advances in optoelectronics technology have occurred since the discovery of a wet thermal oxidation process for selectively converting Al-bearing III–V compound semiconductors to insulating, low index of refraction native oxides.¹ The low index has been employed for various applications including optical mode confinement in edge-emitting lasers and vertical-cavity surface emitting lasers (VCSELs), high-contrast distributed Bragg reflectors (DBRs) for VCSELs, embedded microlenses, birefringent waveguides for phase matching and photonic lattices.² The refractive index of $\text{Al}_x\text{Ga}_{1-x}\text{As}$ native oxides has been measured by single-wavelength ellipsometry ($x = 0.8$, $n = 1.63$ at 633 nm),³ angular Fabry–Pérot spectroscopic analysis ($x = 1$, $n = 1.52$ at $\sim 870\text{ nm}$),⁴ DBR reflectivity simulation ($x = 1$, $n = 1.55$ at $\sim 1000\text{ nm}$),⁵ variable-angle spectroscopic ellipsometry ($x = 0.98$, $n = 1.65$ at 240 nm to 1.56 at 1700 nm),⁶ and spectroscopic ellipsometry ($x = 1$, $n = 1.77$ at 300 nm to 1.66 at 800 nm).⁷ In this letter, we present results from prism coupling measurements on the refractive index of $0.6\text{--}1.4\ \mu\text{m}$ surface-oxidized $\text{Al}_x\text{Ga}_{1-x}\text{As}$ films with data on Al composition ($0.3 \leq x \leq 0.97$), oxidation temperature ($400^\circ\text{C} \leq T \leq 500^\circ\text{C}$), and carrier gas purity dependence. Index stability is monitored over time, revealing hygroscopic behavior.

The heterostructures used in this study were grown on semi-insulating GaAs substrates by metalorganic chemical vapor deposition (MOCVD), and consist of $1\ \mu\text{m}$ thick layers with Al compositions of $x = 0.3, 0.5, 0.7, 0.8$, and 0.9 , controlled to better than ± 0.01 . Two additional samples have $1.4\ \mu\text{m}$ $\text{Al}_{0.4}\text{Ga}_{0.6}\text{As}$, or $0.6\ \mu\text{m}$ $\text{Al}_{0.9}\text{Ga}_{0.03}\text{As}$, oxidation layers. All structures have $500\ \text{Å}$ GaAs cap layers, and all layers are not intentionally doped. After removing the cap layer in a nonselective $1:8:80\ \text{H}_2\text{SO}_4:\text{H}_2\text{O}_2:\text{H}_2\text{O}$ etch, conventional wet-thermal surface oxidation of the $\text{Al}_x\text{Ga}_{1-x}\text{As}$ layers is performed in a 2 in. diam quartz tube furnace with $0.66\ \text{l/min}$ of N_2 bubbled through 95°C H_2O . Typical sample sizes are $\sim 4 \times 4\ \text{mm}^2$. Oxidation in the reaction-rate limited (linear thickness growth) regime is confirmed for x

$= 0.8$ at 475°C and assumed for lower Al compositions and temperatures.

Prism coupling measurements⁸ of refractive index and thickness are performed with a Metricon⁹ Model 2010 instrument at $\lambda = 632.8\ \text{nm}$. While limited to thicker films than can be characterized by ellipsometry, the technique requires no knowledge of substrate index, film absorption, or other fitting parameters. Calibrated with a fused quartz standard ($n = 1.45701$), the index accuracy is ± 0.0001 . Oxidation times are adjusted (from 20 min for $x = 0.9$, 400°C to 696 min for $x = 0.3$, 425°C) to obtain oxide thicknesses sufficient to support typically three optical modes ($d \geq 0.7\ \mu\text{m}$). Care is taken to stop the oxidation front within the AlGaAs layer to obtain uniform index films. The consistency among mode angles for three mode films provides a measure of index homogeneity. The very low standard deviations (typically 0.0005) indicate highly uniform film composition versus depth. This is confirmed for one $x = 0.8$ oxide film by secondary ion mass spectrometry (SIMS) which shows flat Al, Ga, O, and As depth profiles (data not shown). Between 0.633 and $1.55\ \mu\text{m}$ we measure an index decrease on $x = 0.4$ films of just 0.020, comparable to the dispersion measured elsewhere.^{6,7}

The dependence of the refractive index of oxidized $\text{Al}_x\text{Ga}_{1-x}\text{As}$ on the as-grown crystal's Al composition x is shown in Fig. 1(a) for oxidation temperatures of 400, 425, 450, 475, and 500°C . In Fig. 1(b), these data are replotted to more clearly show the dependence of the refractive index on oxidation temperature and carrier gas purity. The lines connecting datum points are only to guide the eye. Solid symbols represent films oxidized with a N_2 carrier gas purity of $\geq 99.999\%$ ($\sim 10\ \text{ppm}\ \text{O}_2$). Each point consists of measurements on an average of nine different samples oxidized in two or three separate oxidation runs. Open symbols correspond to oxidations on a few samples with a lesser N_2 purity ($\leq 99.95\%$, $\geq 300\ \text{ppm}\ \text{O}_2$), and reveal a significant index dependence on carrier gas. Except where indicated otherwise, error bars for each datum point are smaller than the plotted symbols (as represented by the $\pm 1\sigma$ scale for the typical standard deviation of $\sigma = 0.004$). In Fig. 1(a), we also

^{a)}Electronic mail: dhall@nd.edu

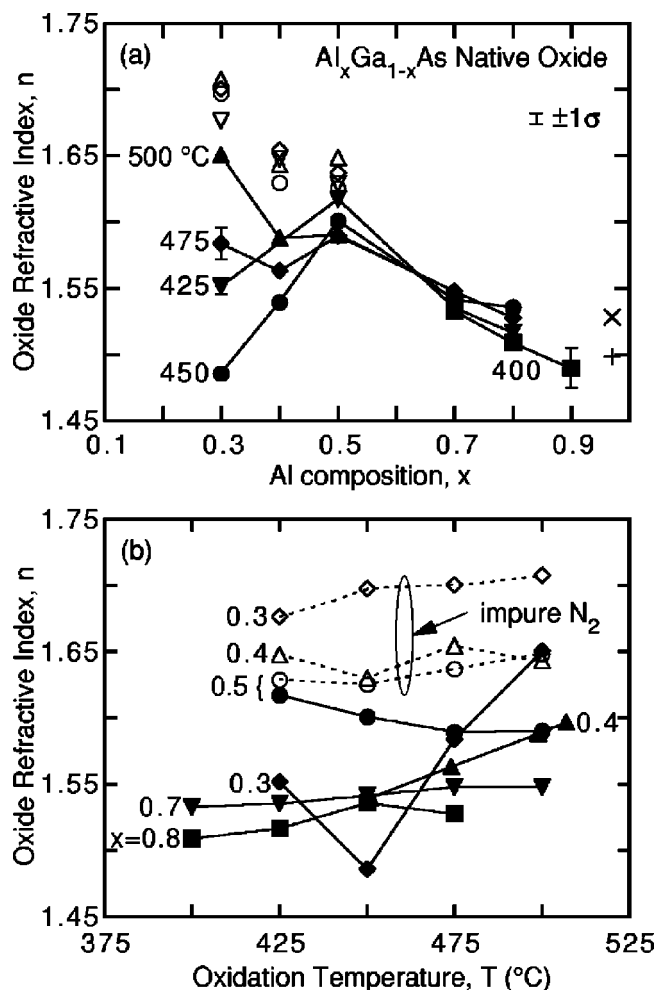


FIG. 1. Dependence of the refractive index of oxidized $\text{Al}_x\text{Ga}_{1-x}\text{As}$ plotted (a) vs Al composition, x , for different oxidation temperatures and (b) vs oxidation temperature for different x values. Oxidations were done in both high purity N_2 (solid symbols) and with ≥ 300 ppm O_2 in the N_2 carrier gas (open symbols). For $x=0.97$, samples are oxidized both from the surface (+) and laterally (\times).

compare $0.6 \mu\text{m}$ thick $\text{Al}_{0.97}\text{Ga}_{0.03}\text{As}$ films fully oxidized (+) from the surface at $400\text{--}430^\circ\text{C}$ ($n=1.498\pm 0.024$) and (\times) laterally along $30 \mu\text{m}$ mesas at $400\text{--}500^\circ\text{C}$ ($n=1.528\pm 0.014$). The higher lateral oxide index may be due to water adsorption (discussed below) during wet chemical etching for cap layer removal prior to measurement, or to a greater density of the by-product As trapped under the more restrictive conditions. The higher standard deviations are due to greater process variation and less controlled, rapid surface oxidations.

Wet oxidized $\text{Al}_x\text{Ga}_{1-x}\text{As}$ ($x \geq 0.8$) has been shown to form an amorphous solid solution of $(\text{Al}_x\text{Ga}_{1-x})_2\text{O}_3$.^{2,10} The decreasing oxide index observed in Fig. 1(a) for $x \geq 0.5$ is consistent with an $(\text{Al}_x\text{Ga}_{1-x})_2\text{O}_3$ film in which lighter Al atoms replace Ga atoms as x increases. As shown in Fig. 1(b), n varies < 0.03 with T for these compositions. However, for $x=0.3$ material n increases $+0.16$ from 450 to 500°C , suggesting a possible oxide chemical phase transition. X-ray diffraction measurements on $x=0.3$ samples oxidized at 450 and 500°C reveal that our films are also completely amorphous. Thus, chemical differences cannot be identified via crystal structure. Elastic recoil detection studies¹⁰ indicate that hydrogen levels are too low for ox-

TABLE I. Refractive index change during storage under ambient room temperature (295 K) and relative humidity ($30\%\text{--}40\%$) conditions.

Starting material	Oxidation temp. ($^\circ\text{C}$)	Initial index	Time (days)	Final index	Index change
$\text{Al}_{0.3}\text{Ga}_{0.7}\text{As}$	450	1.483	804	1.559	+0.076
$\text{Al}_{0.3}\text{Ga}_{0.7}\text{As}$	500	1.651	802	1.712	+0.061
$\text{Al}_{0.7}\text{Ga}_{0.3}\text{As}$	400	1.531	9	1.549	+0.018
$\text{Al}_{0.7}\text{Ga}_{0.3}\text{As}$	400	1.535	888	1.618	+0.083
$\text{Al}_{0.7}\text{Ga}_{0.3}\text{As}$	425	1.535	3	1.544	+0.009
$\text{Al}_{0.7}\text{Ga}_{0.3}\text{As}$	425	1.533	8	1.544	+0.011
$\text{Al}_{0.7}\text{Ga}_{0.3}\text{As}$	425	1.540	55	1.558	+0.018
$\text{Al}_{0.7}\text{Ga}_{0.3}\text{As}$	425	1.535	823	1.604	+0.069
$\text{Al}_{0.7}\text{Ga}_{0.3}\text{As}$	500	1.547	791	1.613	+0.066
$\text{Al}_{0.8}\text{Ga}_{0.2}\text{As}$	425	1.517	819	1.616	+0.099
$\text{Al}_{0.9}\text{Ga}_{0.1}\text{As}$	400	1.465	10	1.488	+0.023

dized AlAs to be a hydroxide phase. However, Ga (like Al) does readily form hydroxides,¹¹ and solid solutions of the hydrates $\text{Al}_2\text{O}_3 \cdot \text{H}_2\text{O}$ and $\text{Ga}_2\text{O}_3 \cdot \text{H}_2\text{O}$ also exist.¹² Such hydroxides are less dense and consequently have substantially lower refractive indices.¹³ The Ga monohydroxide $\text{GaO}(\text{OH})$ is the most stable, and is converted when heated to $420\text{--}500^\circ\text{C}$ into Ga_2O_3 .¹¹ It is thus likely that the low index values observed in Fig. 1 for $x \leq 0.4$ are due to the formation of an amorphous solid solution resembling the hydroxide $\text{Al}_x\text{Ga}_{1-x}\text{O}(\text{OH})$ [i.e., $(\text{Al}_x\text{Ga}_{1-x})_2\text{O}_3 \cdot \text{H}_2\text{O}$], which transitions to $(\text{Al}_x\text{Ga}_{1-x})_2\text{O}_3$ at higher temperatures.

Data in Fig. 1 also show that the index of $\text{Al}_{0.3}\text{Ga}_{0.7}\text{As}$ oxides formed with lower purity (greater O_2 content) N_2 carrier gas is substantially higher ($\Delta n=0.06\text{--}0.27$) and less temperature dependent. This can be attributed to increased thermodynamic favorability for the formation of the denser and more stable $(\text{Al}_x\text{Ga}_{1-x})_2\text{O}_3$ phase in the presence of additional O_2 . Oxidation reactions for AlGaAs are known to vary substantially with Al composition and oxidizing environment. The wet-thermal oxidation reaction converting AlAs to Al_2O_3 becomes thermodynamically unfavorable ($\Delta G^{698} = +10 \text{ kJ/mol}$) when Al is replaced with Ga, accounting for the high Al selectivity in oxidation rate.² However, in a dry O_2 environment, the oxidation rate of $\text{Al}_x\text{Ga}_{1-x}\text{As}$ has been shown to increase as the Al content decreases (for $x \leq 0.52$, $T \geq 550^\circ\text{C}$).¹⁴ Using a pure O_2 carrier gas bubbled through H_2O completely suppresses the oxidation of $\text{Al}_{0.98}\text{Ga}_{0.02}\text{As}$.² However, the addition of just 0.1% (1000 ppm) O_2 to a N_2 carrier gas significantly reduces the reaction-rate activation energy and enhances oxidation rates for $\text{Al}_{0.6}\text{Ga}_{0.4}\text{As}$, but has very little effect on $\text{Al}_{0.77}\text{Ga}_{0.23}\text{As}$.¹⁵ We too observe with lower purity N_2 that the oxidation rates for $x \leq 0.5$ increase and activation energies decrease.

These results suggest that as x decreases, added O_2 is needed during wet oxidation to obtain the denser, higher index $(\text{Al}_x\text{Ga}_{1-x})_2\text{O}_3$ in preference to $\text{Al}_x\text{Ga}_{1-x}\text{O}(\text{OH})$. We note that data for $x=0.4$ and 0.5 films show a similar, but smaller, sensitivity to an increased O_2 content in the N_2 carrier gas as the Ga content in the films decreases. The index versus composition data for $x \leq 0.5$ and lower purity N_2 in Fig. 1(a) are nearer to expected values for $(\text{Al}_x\text{Ga}_{1-x})_2\text{O}_3$ based on reported indices for stoichiometric Ga_2O_3 films of $1.84\text{--}1.88$.¹⁶ The exact O_2 content in our lower purity N_2 was not controlled, and the full dependence of index on O_2

TABLE II. Refractive index change during exposure to 100% relative humidity (295 K).

Starting material	Oxidation temp. (°C)	Initial index	Time (days)	Final index	Index change
Al _{0.3} Ga _{0.7} As	450	1.483	3	1.551	+0.068
Al _{0.3} Ga _{0.7} As	450	1.713	3	1.742	+0.029
Al _{0.3} Ga _{0.7} As	500	1.642	3	1.689	+0.047
Al _{0.8} Ga _{0.2} As	400	1.509	3	1.607	+0.098
Al _{0.9} Ga _{0.1} As	400	1.497	3	1.571	+0.074

content requires further study. For the $x=0.4$ impure N₂ data in Fig. 1(b), the lower index values at 450 and 500 °C correlate with lower oxidation rates, consistent with a drop in O₂ content for these runs. Although an O₂ content of 20% results in surface roughening,¹⁵ we observe smooth, specular surfaces with the lower O₂ levels that produce our higher index films.

Data on the refractive index variation with time following oxidation are summarized in Table I for several oxidized samples stored in ambient room temperature and relative humidity (RH) conditions. We have observed positive index drifts of up to 0.10 (6.6%) over a period of ~800 days, a time by which the index is believed to have stabilized. For consistency, all data in Fig. 1 were measured immediately after oxidation. We attribute this instability to adsorption of moisture by a porous oxide, with a possible further chemical reaction with the adsorbed moisture. Samples monitored for 15 days while stored in a desiccator at 0% RH showed 85–93% as much drift as those stored in ambient conditions (data not shown). This suggests the oxide film chemistry may evolve through reactions with existing moisture trapped either during wet oxidation or the initial measurement period.

The likelihood of additional moisture adsorption from the air is supported by the observation of accelerated index drift in the presence of 100% RH (Table II). By the end of ~3 days, index drift saturates at levels comparable to those observed in Table I. Attempts to dry the samples of Table II and reverse the index drift were largely unsuccessful. Progressively aggressive bakes culminating with 12 h at 160 °C decreased the index of the fourth sample just –0.017 to 1.590. While it is possible that a more effective drying technique is needed, these data may indicate that a further chemical reaction has occurred, possibly involving residual As² or less stable Ga hydroxides. We note that, for all samples, no oxide thickness variations are observed outside our ±1% measurement standard deviation.

We have also separately annealed five fully oxidized samples ($x=0.5$, 500 °C, 2 h) for 60–80 min in Ar at $T=400$ –800 °C. Before annealing, their mean index increased during ~400 days in ambient air by 0.054 from 1.591 to 1.645. Upon annealing, the index decreases 0.044 at 400 °C, 0.047 (500), 0.056 (600), 0.093 (700), and 0.100 (800). The larger index decrease above the sublimation temperature of As (613 °C) suggests the drop may be due to the removal of residual As.

Data in Table I for $x=0.7$ indicate that films oxidized at 400 °C are somewhat more hygroscopic than films oxidized at ≥425 °C. Index values at four different times for $x=0.7$, 425 °C oxides demonstrate a sublinear (saturating) increase. The higher-index $x=0.3$ films formed at 500 vs 450 °C (high purity N₂) are denser and more stable. The densest oxide in Table II ($x=0.3$, 450 °C, $n_i=1.713$) was oxidized in lower purity N₂ and has the smallest index drift (+0.029, ~43% of the low index, high purity N₂ sample), having nearly saturated at 0.028 in 1 day. High purity N₂ was used for all other samples in both tables. It is unclear whether this increased index stability is due to less moisture adsorption by the denser, less porous film, or to a more chemically stable oxide phase that reacts less with adsorbed moisture.

In conclusion, we have characterized variations in the refractive index of wet oxidized AlGaAs with composition, oxidation temperature, and carrier gas purity. The index is found to vary up to 7% over time due to adsorbed moisture which may further react with the oxides. Denser, more stable native oxides of Al_{*x*}Ga_{1–*x*}As ($x\leq 0.5$) are obtained when a small amount of O₂ is present in the carrier gas. Further material analysis is required to fully understand the nature of the index changes observed.

The authors gratefully acknowledge the support of J. H. Jackson of Metricon Corp. and NSF CAREER Award No. ECS-9502705, and thank S. C. Sevov for performing x-ray diffraction measurements.

- J. M. Dallesasse, N. Holonyak, Jr., A. R. Sugg, T. A. Richard, and N. El-Zein, Appl. Phys. Lett. **57**, 2844 (1990).
- See K. D. Choquette, K. M. Geib, C. I. H. Ashby, R. D. Twesten, O. Blum, H. Q. Hou, D. M. Follstaedt, B. E. Hammons, D. Mathes, and R. Hull, IEEE J. Sel. Top. Quantum Electron. **3**, 916 (1997).
- A. R. Sugg, E. I. Chen, N. Holonyak, Jr., K. C. Hsieh, J. E. Baker, and N. Finnegan, J. Appl. Phys. **74**, 3880 (1993).
- P. Heremans, M. Kuijck, R. Windisch, J. Vanderhaegen, H. D. Neve, R. Vounckx, and G. Borghs, J. Appl. Phys. **82**, 5265 (1997).
- M. H. MacDougal, P. D. Dapkus, A. E. Bond, C.-K. Lin, and J. Geske, IEEE J. Sel. Top. Quantum Electron. **3**, 905 (1997).
- K. J. Knopp, R. P. Mirin, D. H. Christensen, K. A. Bertness, A. Roshko, and R. A. Synowicki, Appl. Phys. Lett. **73**, 3512 (1998).
- A. Bek, A. Aydinli, J. G. Champlain, R. Naone, and N. Dagli, IEEE Photonics Technol. Lett. **11**, 436 (1999).
- P. K. Tien and R. Ulrich, J. Opt. Soc. Am. **60**, 1325 (1970).
- Metricon Corp., Pennington, NJ 08534.
- R. D. Twesten, D. M. Follstaedt, and K. D. Choquette, in *Vertical-Cavity Surface Emitting Lasers*, edited by K. D. Choquette and D. G. Deppe [Proc. SPIE **3003**, 55 (1997)].
- I. A. Sheka, I. S. Chaus, and T. T. Mityureva, *The Chemistry of Gallium* (Elsevier, New York, 1966), pp. 41–43.
- V. G. Hill, R. Roy, and E. F. Osborn, J. Am. Ceram. Soc. **35**, 135 (1952).
- C. Misra, *Industrial Alumina Chemicals* (American Chemical Society, Washington, D.C., 1986), p. 12.
- J. Shin, K. M. Geib, C. W. Wilmsen, P. Chu, and H. H. Wieder, J. Vac. Sci. Technol. A **9**, 1029 (1991).
- R. S. Burton and T. E. Schlesinger, J. Appl. Phys. **76**, 5503 (1994).
- M. Passlack, E. F. Schubert, W. S. Hobson, M. Hong, N. Moriya, S. N. G. Chu, K. Konstadinidis, J. P. Mannaerts, M. L. Schnoes, and G. J. Zyzdik, J. Appl. Phys. **77**, 686 (1995).